Nuclear Engineering and Technology 50 (2018) 751–757

Contents lists available at ScienceDirect

Nuclear Engineering and Technology

journal homepage: www.elsevier.com/locate/net

Original Article

Design and construction of a new ultraviolet sensor using CsI deposition in the ionization chamber

R. Souri [a, d, *], A. Negarestani [b], S. Souri [c], M. Farzan [d], M. Mahani [a]

[a] Faculty of Science and Modern Technology, Graduate University of Advanced Technology, Kerman, Iran
[b] Faculty of Electrical and Computer Engineering, Graduate University of Advanced Technology, Kerman, Iran
[c] Department of Energy Engineering and Physics, Amirkabir University of Technology, Tehran, Iran
[d] Department of Physics, Izeh Branch, Islamic Azad University, Izeh, Iran

A R T I C L E I N F O

Article history:
Received 8 August 2016
Received in revised form
13 March 2018
Accepted 25 March 2018
Available online 11 April 2018

Keywords:
CsI Photocathode
Fire Sensor
Ion Chamber
UV Detector

A B S T R A C T

In this article, a UV sensor that is an appropriate tool for fire detection has been designed and constructed. The structure of this UV sensor is an air-filled single-wire detector that is able to operate under normal air condition. A reflective CsI photocathode is installed at the end of the sensor chamber to generate photoelectrons in the ion chamber. An electric current is produced by accelerating photoelectrons to the anode in the electric field. The detector is able to measure the intensity of the incident UV rays whenever the current is sufficiently high. Therefore, the sensitivity coefficient of this sensor is found to be 7.67×10^{-6} V/photons/sec.

1. Introduction

Forest fires are considered a significant issue all around the world because of their impact on human life and the environment. In more detail, the area damaged by fire in five European countries in the last 35 years (between 1980 and 2014) has been indicated in Table 1 [1]. The statistical data for other countries can be seen in the studies by van Lierop et al. and Churches et al. [2,3]. Recently, the risk of forest fires has increased as a consequence of climate change and human activity. The most efficient and effective method to avoid the spread of forest fires is the immediate detection of the initial flame. Various methods including two main categories are currently available for flame detection at the beginning of a fire; the first category is flame detection by the use of an infrared (IR) radiation emission detector; the second is smoke and fire detection by unaided eyes [4].

To detect IR radiation from a fire, IR detectors are installed in satellites and small aircraft [5]. It has been proven that this type of detector has several problems, such as limited detection area, clouds that act as a barrier to watch for fires, reach of IR detector, and the high cost of IR cameras. To achieve better and more accurate results than those possible using IR detection, gas detectors are used. This system detects UV photons emitted from flames; so, it is more efficient.

Gas detectors operate on the basis of intense electric field generation in small areas. UV photons enter the device and reach the photocathode. If photon energy is sufficient to ionize the photocathode, generated electrons are accelerated to anode by intense electric field. As a result, incident electrons to anode are measured as the electric current.

In this study, a single-wire structure for UV flame sensors, which are the most efficient among the numerous types of UV detectors, has been used [6]. This type of sensor has already been of interest; for instance, Roger E. Axmark et al. recorded their invention with a US Patent entitled “Flame Detector Utilizing an Ultraviolet Sensitive Geiger Tube” in 1967 [7]. This simple structure, used as a UV flame detector, operates in the Geiger–Muller region.

The output pulse amplitude of the Geiger–Muller detector is large. Therefore, this output, produced by simple circuit, can be used to measure UV photons without any amplifier. However, the major problem of Geiger–Muller detectors is their long dead time. Therefore, this type of detector is restricted to low count rate (about 10^3–10^4 pulses/sec). Moreover, Geiger–Muller detectors also have a limited lifetime. To solve this problem, detectors operated in the

* Corresponding author.
E-mail address: razisouri1@gmail.com (R. Souri).

https://doi.org/10.1016/j.net.2018.03.018

Table 1
Number of fires and burnt area in the five Southern European countries in the last 35 years [1].

Number of fires	Portugal	Spain	France	Italy	Greece[a]	Total
2014	**7 067**	**9 771**	**2 778**	**3 257**	**552**	**23 425**
Percentage of total in 2014	30%	42%	12%	14%	2%	100%
Average 1980–1989	7 381	9 515	4 910	11 575	1 264	34 645
Average 1990–1999	22 250	18 152	5 538	11 164	1 748	58 851
Average 2000–2009	24 949	18 369	4 418	7 259	1 695	56 690
Average 2010–2014	18 956	13 207	3 416	5 502	1 128	42 209
Average 1980–2014	18 302	15 040	4 735	9 357	1 506	48 940
TOTAL (1980–2014)	640 586	526 390	165 737	327 487	52 696	1 712 896
Burnt areas (ha)	**Portugal**	**Spain**	**France**	**Italy**	**Greece**	**Total**
2014	**19 929**	**46 721**	**7 493**	**36 125**	**25 846**	**136 114**
Percentage of total in 2014	15%	34%	6%	27%	19%	100%
Average 1980–1989	73 484	244 788	39 157	147 150	52 417	556 995
Average 1990–1999	102 203	161 319	22 735	118 573	44 108	448 938
Average 2000–2009	150 101	127 229	22 362	83 878	49 238	432 809
Average 2010–2014	97 964	97 752	8 504	62 911	34 111	301 243
Average 1980–2014	107 077	166 346	25 287	108 873	46 519	454 104
TOTAL (1980–2014)	3 747 705	5 822 123	885 056	3 810 561	1 628 181	15 893 626

[a] Numbers of fires are incomplete since 2009 [1].

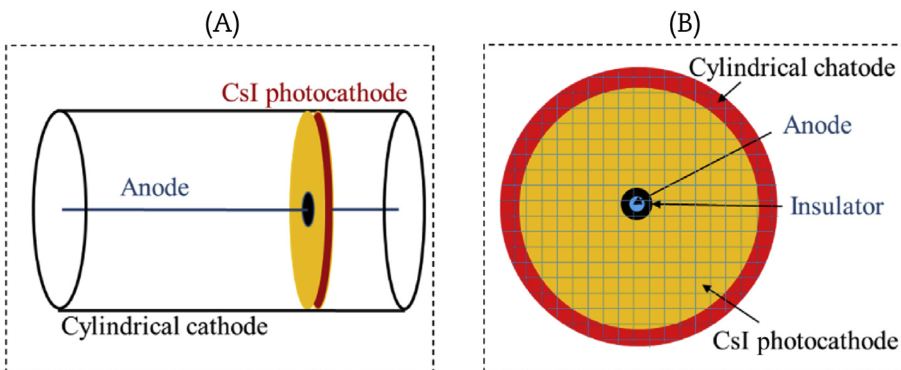

Fig. 1. Schematic diagram. (A) Detector chamber. (B) Cross face of detector.

Table 2
The dimensions of the UV detector components.

Component	Material	Diameter	Height
Chamber	Stainless steel (SSL)	5.4 cm	20 cm
Anode	Steel	2 mm	15 cm

ionization region instead of in the Geiger–Muller region are proposed.

In comparison with Geiger–Muller counters, ion-chamber detectors operate in the current mode, in which there is no dead time or any lifetime limitation [8]. In addition, to achieve the required field for a single-wire anode with 0.1-mm diameter, the operating voltage of the Geiger–Muller tubes is about 500–2000 V at the condition of normal gases at pressures of several tenths of an atmosphere [8]. On the other hand, our detector is designed to have the ability to operate under normal air condition. In addition, no high voltage (HV) source is required for optimized detector performance. These features have made our designed detector economically feasible.

The main application of our designed UV detector is determination of actual fire expansion and intensity, for which

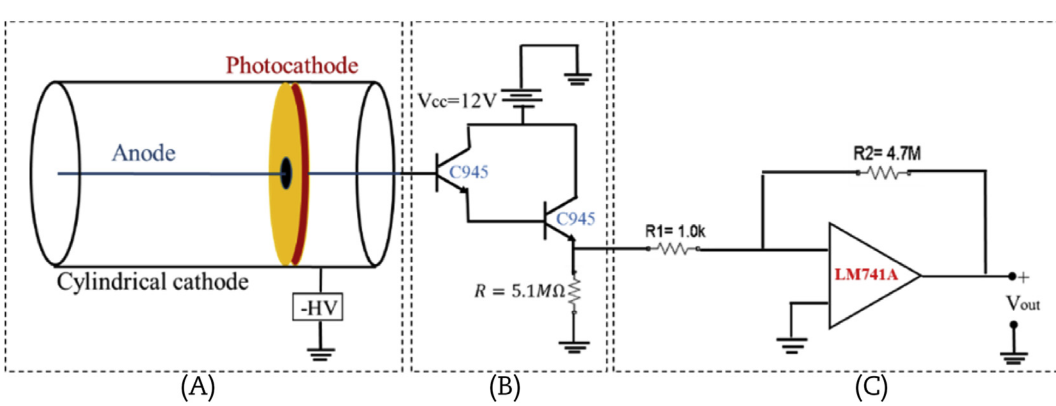

Fig. 2. (A) Detector chamber. (B) Preamplifier circuit that is located at the end of the cylinder chamber. (C) Amplifier circuit.

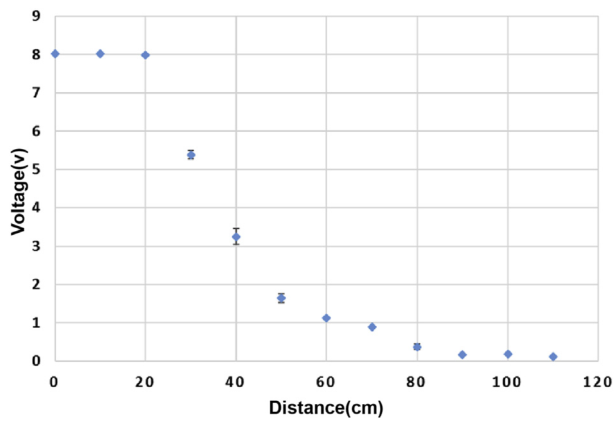

Fig. 3. The measured output voltage versus distance between the candle flame and detector in normal air.

Geiger–Muller detectors fail because of their dead time. This detector can be extensively used because of its simple design. Interestingly, the power consumption of this detector is low so that it can even start to operate with ordinary solar cells (12 V). It is worth mentioning that we believe that the best method of fire detection is the simultaneous use of an ionization chamber and a Geiger–Muller detector. This structure is also used to measure the neutron flux in nuclear reactors, where the BF3 tube and fission production chamber operate in Geiger–Muller and ion-chamber modes, respectively.

Comparing with the Geiger–Muller detector and other kinds of detectors (proportional types), the designed UV detector has other advantages in its ability to work under normal air condition (air-filled single-wire detector) and to work at higher rates.

2. Detector design

To detect UV rays in the range of the UV emission from fires, the ion-chamber detector is designed and constructed. Fig. 1 provides a schematic drawing of the UV detector. The detector consists of a stainless steel cylinder and a direct wire that is located at the center of the cylinder as the ion chamber and anode, respectively. Table 2 provides information about the dimensions of the detector components.

As can be seen in Fig. 1, the reflective photocathode is installed at the end of the chamber and connected to the HV (Fig. 2A). Using a suitable insulator, this photocathode is isolated from the anode that crossed through the center of the cathode. The photocathode is made of a cesium iodide compound (CsI) layer placed on a circular copper substrate with diameter equal to the chamber inner diameter.

The process of CsI photoionization is described by Equation (1):

$$h\nu + CsI \rightarrow Cs^{+} + I + e^{-} \tag{1}$$

According to Equation (1), photoelectrons are generated when UV rays are collected by CsI with the same absorption spectrum as UV rays emitted from the fire.

2.1. Construction of photocathode

Photocathodes can be constructed as either opaque (reflective) or semitransparent layers [8]. Each type is used in a specific geometric arrangement. In this study, a reflective photocathode has been constructed with regard to our detector structure. In a conventional reflective photocathode, the thickness is slightly larger than the maximum escape depth, and the device is supported by a thick shielding material.

The procedure used for CsI deposition on a metallic substrate has several stages. Primarily, a solution consisting of a sufficient amount of CsI in distilled water is prepared and sprayed over the preheated copper using a nebulizer, repeatedly. The copper substrate is heated to 60–70°C in each interval to facilitate the evaporation of solvent. Finally, a uniform CsI layer is deposited on the substrate at atmospheric pressure, while there is no need of any special vacuum equipment. To ensure the uniformity of the deposited layer, the spraying distance from the substrate should be kept constant all over its area. Furthermore, the thickness of the deposited layer can be simply controlled by the number of spraying and heating cycles [9].

As reported in the studies by Garai Baishali et al. [10] and Shalem [11], the thickness of 300 nm is an appropriate value for conventional reflective photocathodes. Therefore, the parameters of the CsI are chosen in such a way that a 300-nm CsI layer will be produced. Moreover, to ensure the uniformity of the CsI layer, the photocathode layer is analyzed using an accurate microscope. The observations prove that the layer is uniform.

2.2. Design of electronic circuits

In comparison with Geiger–Muller tubes and proportional detectors, this detector's ionization chamber required less applied HV. Here, the ordinary battery voltage of 12 V is fed to the HV circuit, and an output voltage of −250 V is generated and applied between anode and cathode.

To measure the ionization current by counting the photoelectrons emitted from CsI in the chamber, an electrical circuit consisting of a preamplifier and amplifier was designed and constructed. Fig. 2B illustrates the preamplifier circuit, located at the end of the chamber exactly after the anode. The key factor in the design of the preamplifier is the minimization of the distance between the anode and preamplifier, performed to reduce noise.

In the preamplifier, two transistors are used and connected to each other by Darlington method to amplify the ionization current by a factor of 10^4. Then, this amplified current passes through $5.1 M\Omega$ resistance. In the next stage, the voltage across this resistance is amplified by an operation amplifier (Model: LM741A), as shown in Fig. 2C. The amplification factor of this amplifier is $4.7 \times 10^3 \left(\approx R_2/R_1\right)$, set by choosing $R_1 = 1 k\Omega$ and $R_2 = 4.7 M\Omega$. Therefore, the ratio of the output voltage to the chamber current, or gain (G), is equal to 230 (mV/pA).

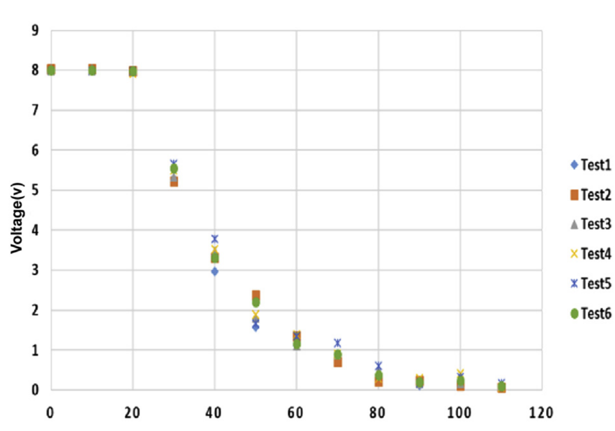

Fig. 4. Repetition test for 6 times at 2 weeks after photocathode deposition.

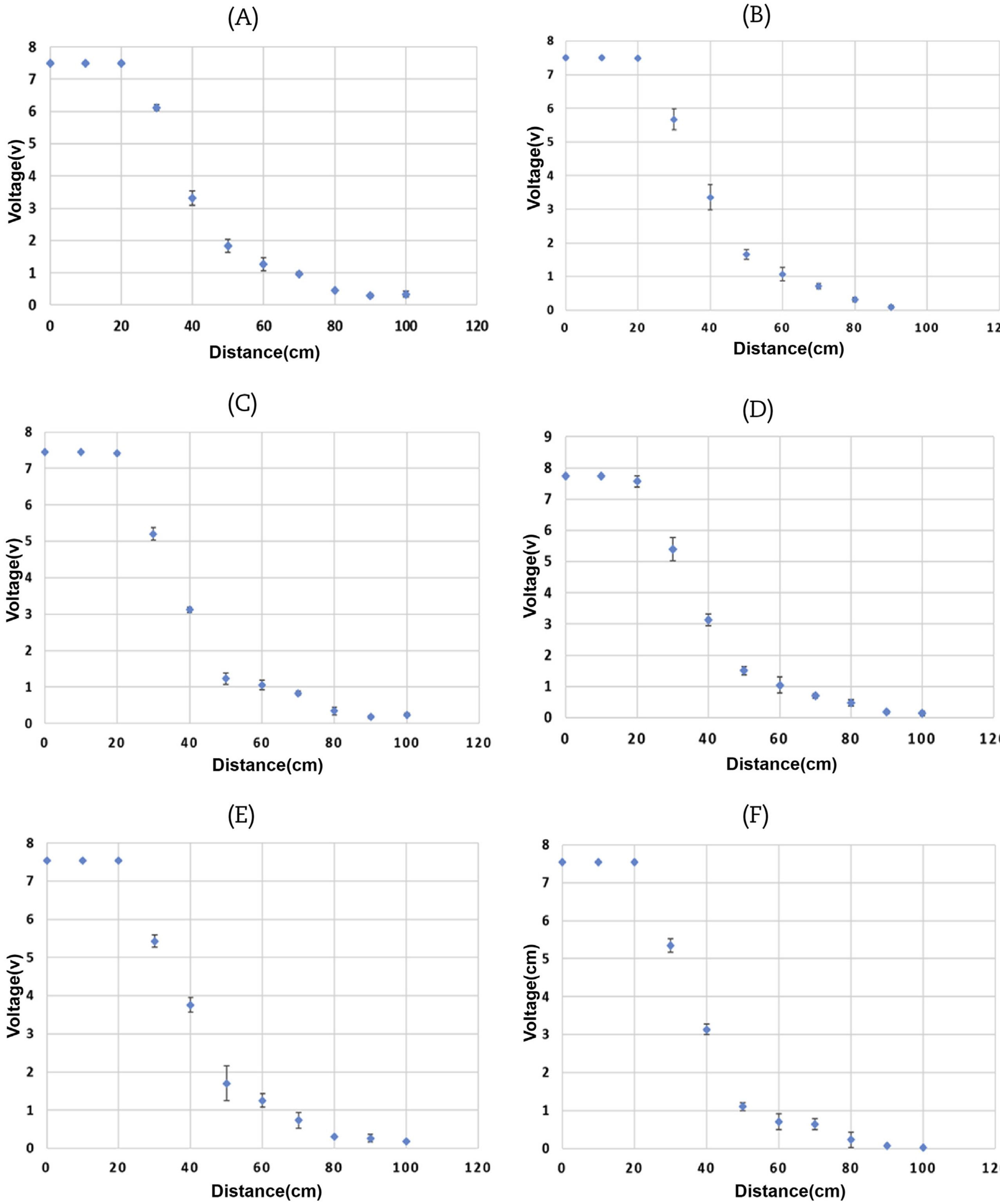

Fig. 5. The output voltage versus distance between the candle flame and external aperture of the detector chamber at different time intervals from deposition. (A) 4 weeks after deposition. (B) 6 weeks after deposition. (C) 8 weeks after deposition. (D) 16 weeks after deposition. (E) 20 weeks after deposition. (F) 24 weeks after deposition.

One of the most significant parameters of the detector is the device sensitivity, which is calculated from the output voltage by Equation (2):

$$V_{out} = I \times q_e \times G \times \beta \tag{2}$$

where I is the UV radiation intensity (the number of photons reaching the CsI photocathode per second), q_e is the electron charge, G is the gain of the detector, and β is normal photocathode quantum efficiency. The value of β is about 20%, approximately [8]. Therefore, the intrinsic efficiency per photon is $\frac{V_{out}}{I(=1photon/s)} = 7.76 \times 10^{-6}$.

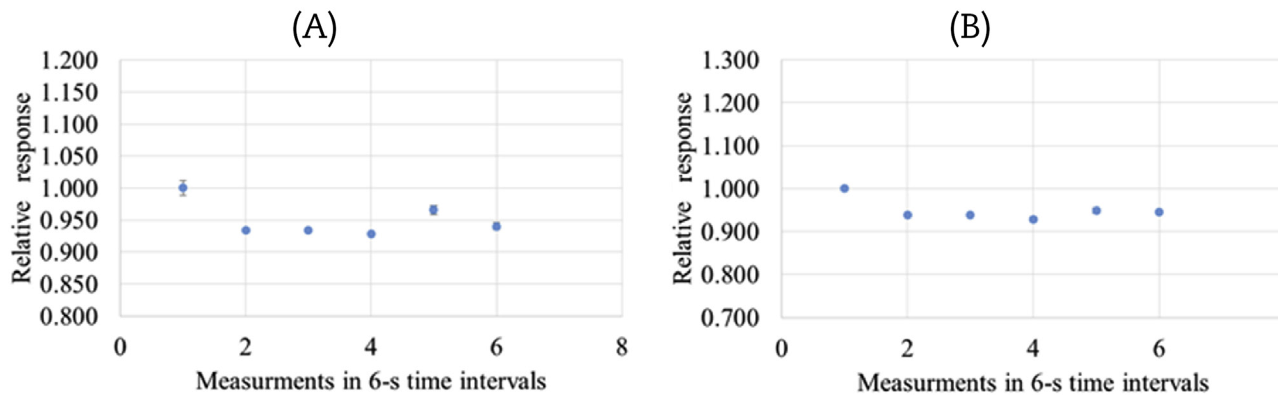

Fig. 6. The output voltage variance at 6-s time intervals (at 2, 4, 6, 8, 16, and 20 weeks after deposition). (A) Distance between the candle flame and detector is 10 cm. (B) Distance between the candle flame and detector is 20 cm.

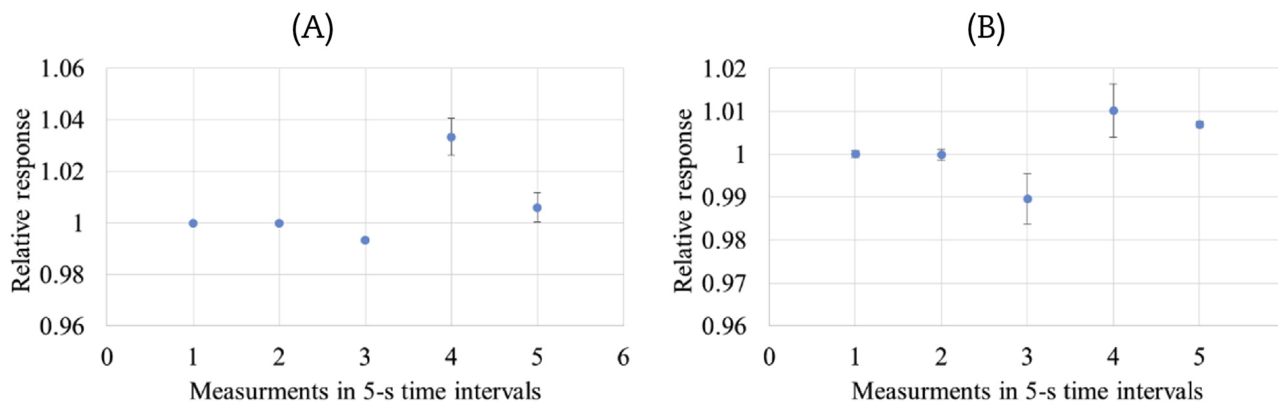

Fig. 7. The variance of output voltage in different time intervals at 4, 6, 8, 16, and 20 weeks after deposition. (A) The variance of output voltage for 10 cm between the candle flame and detector. (B) The variance of output voltage for 20 cm distance between the candle flame and detector.

The efficiency can be calculated from Equation (3):

$$I = FI' \tag{3}$$

where I′ is the total number of photons generated from fire and F is the efficiency. The efficiency, F, is dependent on the presence of a solid angle between the detector and flame. The solid angle is obtained from Equation (4):

$$\Omega = \pi d^2 / R^2 \tag{4}$$

where Ω is a solid angle, d is the detector diameter, and R represents the distance between the detector and flame. Note that Equation (4) is valid at d << R.

3. Results and discussion

The performance of the constructed UV sensor was evaluated in the laboratory by measuring the output voltage needed to detect a candle flame in different conditions. Fig. 3 illustrates the output voltage of the circuit that is obtained and repeated three times for various distances, after photocathode deposition. As can be seen from Fig. 3, there is a remarkable decrease in the output voltage over long distance (more than 20 cm), whereas the UV detector is saturated for short distances (less than 20 cm). For distances more than 20 cm, the variation of the output voltage is approximately proportional to $1/R^2$, where R is the distance of the small flame from the external aperture of the detector chamber.

To obtain the detector sensitivity, the output voltage is calculated for the entrance of one photon per second reaching the CsI in the ion chamber, using Equation (2). Therefore, the sensitivity of this air-filled single-wire detector is obtained at 7.67×10^{-6} V/photons/sec for normal photocathode quantum efficiency. The minimum value of measurable voltage is 10 mV. Thus, the UV sensor should collect at least 1,350 photons/sec to detect UV radiation of a flame.

In the following, the stability of this device is measured for the long and short term.

3.1. Short-term stability tests

In the short-term stability test, the new UV sensor is irradiated six times using a candle flame. After reaching a stabilized state, within a 20-minute interval, the amount of output voltage is measured. After stopping the irradiation and waiting a few minutes, the same process will be repeated generally in six trials. Fig. 4 illustrates the results of the repetition test at 2 weeks after CsI photocathode deposition. Fig. 4 shows that all results are approximately identical for each of the six times of irradiation measurement. Moreover, the obtained experimental data show the same trends in all tests (Fig. 4). In other words, the output voltage is inversely proportional to the square of the distance between the flame and detector.

3.2. Long-term stability tests

To investigate the stability of the deposited CsI layer over time, the same detecting procedure was performed on the CsI photocathode at 4, 6, 8, 16, 20, and 24 weeks after deposition. The results

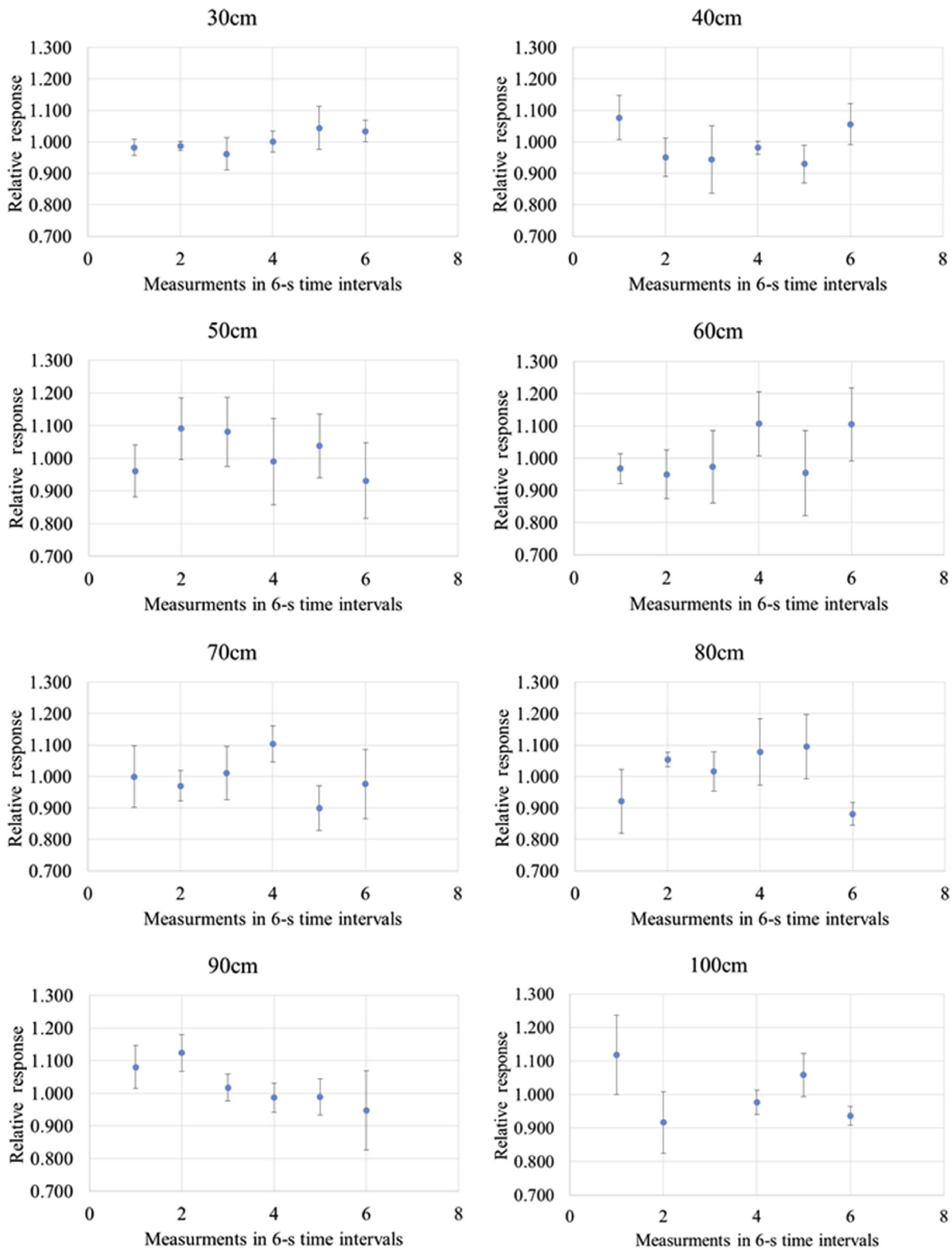

Fig. 8. The output voltage variance at 6-s time intervals (at 2, 4, 6, 8, 16, and 20 weeks after deposition) in different distances between the candle flame and detector.

are shown in Fig. 5, which shows that the output voltage behavior in terms of the distance is approximately constant at all time intervals.

Furthermore, to explore the stability of the UV sensor for different distances between the candle flame and detector, the ion chamber was irradiated six times at different time intervals. The value of the output voltage was measured in a stabilized test between 6-s intervals. Fig. 6 illustrates the variance of the output voltage at distances of 10 cm and 20 cm. As can be seen in Fig. 6, there is a decrease of 6.5% at 4 weeks after deposition. This downward trend is nearly constant at later times.

For further understanding, the output voltage values for distances of 10 cm and 20 cm at different time intervals after 4 weeks are measured. The results are shown in Fig. 7. As can be seen from Fig. 7A and B, the relative responses are less than 3.3% and 1% for 10 cm and 20 cm, respectively. Although there is some fluctuation in the output voltage, the output voltage for the saturated detector ($R < 20$ cm) changed just slightly for different time intervals and various distances between the flame and detector (i.e., 10 cm and 20 cm). (See Fig. 5). In addition, from Fig. 7, it can be clearly seen that the CsI photocathode is stable even under the normal air condition after 4 weeks.

Fig. 8 shows the detector responses at unsaturated distances ($R > 20$ cm). As can be seen in Fig. 8, the fluctuation of these data is greater than the results for the saturated distances. However, the output voltage is still inversely proportional to the square of the distance between the flame and detector (See Fig. 5).

4. Conclusions

In this work, a new type of UV sensor based on an ion chamber has been designed and constructed. In this detector, CsI deposition on a copper substrate is prepared as reflective photocathode, which is installed at the end of the ion chamber.

To measure the output of the system, a preamplifier and amplifier are also designed and constructed.

The main advantage of this constructed detector is its operation under normal air condition. Moreover, this air-filled single-wire detector, which has a nonlimited lifetime, works in very high rates.

The results for short- and long-term stability indicate acceptable repeatability of the UV sensor and show that the output voltage is proportional to the inverse square of the distance. Moreover, the output voltage variance is less than 3.3%. As a consequence, a stable air-filled single-wire detector with a CsI photocathode under normal air condition is constructed and can also be used in other fields in industry, such as in glowing torches.

Conflict of interest

The authors declare no conflict of interest.

Acknowledgments

The authors would like to acknowledge Mr Ali asghar Adibi-Sedeh for sharing his wisdom during this research.

Appendix A. Supplementary data

Supplementary data related to this article can be found at https://doi.org/10.1016/j.net.2018.03.018.

References

[1] G. Schmuck, J. San-Miguel-Ayanz, A. Camia, T. Durrant, R. Boca, G. Libertá, T. Petroliagkis, M. Di Leo, D. Rodrigues, F. Boccacci, Forest fires in Europe, Middle East and North Africa 2014, Technical Report, Joint Research Centre, 2015, https://doi.org/10.2788/224527.
[2] P. van Lierop, E. Lindquist, S. Sathyapala, G. Franceschini, Global forest area disturbance from fire, insect pests, diseases and severe weather events, For. Ecol. Manag. 352 (2015) 78–88.
[3] C.E. Churches, P.J. Wampler, W. Sun, A.J. Smith, Evaluation of forest cover estimates for Haiti using supervised classification of Landsat data, Int. J. Appl. Earth. Obs. Geoinf. 30 (2014) 203–216.
[4] E. Kührt, T. Behnke, H. Jahn, H. Hetzheim, J. Knollenberg, V. Mertens, G. Schlotzhauer, B. Götze, Autonomous early warning system for forest fires tested in Brandenburg (Germany), Int. For. Fire News 22 (2000) 84–90.
[5] A.A. Alkhatib, A review on forest fire detection techniques, Int. J. Distributed Sens. Netw. 2014 (2014).
[6] G. Charpak, P. Benaben, P. Breuil, P. Martinengo, E. Nappi, V. Peskov, Progress in the development of an S-RETGEM-based detector for an early forest fire warning system, J. Instrum. 4 (12) (2009) P12007.
[7] R. E. Axmark, Flame detector utilizing an ultraviolet sensitive Geiger tube, U.S. Patent 3,342,995, issued September 19 (1967).
[8] G.F. Knoll, Radiation Detection and Measurement, John Wiley & Sons, 2010.
[9] D.F. Anderson, S. Kwan, V. Peskov, CsI Photocathode QE and a simple production technique, Nucl. Instrum. Methods Phys. Res. Sect. A Accel. Spectrom. Detect. Assoc. Equip. 326 (3) (1993) 611–612.
[10] Baishali Garai, V. Radhakrishna, K. Rajanna, Effect of vacuum treatment on CsI photocathode performance in UV photon detectors, Opt. Mater. Express 3.7 (2013) 948–953.
[11] C. Shalem, et al., Advances in thick GEM-like gaseous electron multipliers—Part I: atmospheric pressure operation, Nucl. Instrum. Methods Phys. Res. Sect. A Accel. Spectrom. Detect. Assoc. Equip. 558 (2) (2006) 475–489.